

3RL MR 2731

BRL

AD

AD A 037338

MEMORANDUM REPORT NO. 2731

(Supersedes IMR No. 537)

NR

ANGULAR MOTION OF PROJECTILES WITH A
MOVING INTERNAL PART

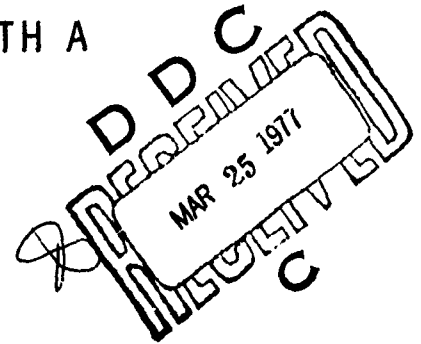
Charles H. Murphy

February 1977

Approved for public release; distribution unlimited.

USA BALLISTIC RESEARCH LABORATORY
ABERDEEN PROVING GROUND, MARYLAND

DDC FILE COPY



Destroy this report when it is no longer needed.
Do not return it to the originator.

Secondary distribution of this report by originating
or sponsoring activity is prohibited.

Additional copies of this report may be obtained
from the National Technical Information Service,
U.S. Department of Commerce, Springfield, Virginia
22151.

The findings in this report are not to be construed as
an official Department of the Army position, unless
so designated by other authorized documents.

UNCLASSIFIED

SECURITY CLASSIFICATION OF THIS PAGE (When Data Entered)

REPORT DOCUMENTATION PAGE		READ INSTRUCTIONS BEFORE COMPLETING FORM
1. REPORT NUMBER BRL Memorandum Report No. 2731	2. GOVT ACCESSION NO.	3. RECIPIENT'S CATALOG NUMBER
4. TITLE (and Subtitle) ANGULAR MOTION OF PROJECTILES WITH A MOVING INTERNAL PART	5. TYPE OF REPORT & PERIOD COVERED Final rept.	6. PERFORMING ORG. REPORT NUMBER
7. AUTHOR(s) Charles H. Murphy	8. CONTRACT OR GRANT NUMBER(s)	
9. PERFORMING ORGANIZATION NAME AND ADDRESS US Army Ballistic Research Laboratory Aberdeen Proving Ground, Maryland 21005	10. PROGRAM ELEMENT, PROJECT, TASK AREA & WORK UNIT NUMBERS RDT&E/1L161102AH43	
11. CONTROLLING OFFICE NAME AND ADDRESS US Army Materiel Development and Readiness Command 5001 Eisenhower Avenue Alexandria, Virginia 22333	12. REPORT DATE FEBRUARY 1977	
13. MONITORING AGENCY NAME & ADDRESS (if different from Controlling Office) BRL-MR-2731	14. NUMBER OF PAGES 59	
15. SECURITY CLASS. (of this report) UNCLASSIFIED		15a. DECLASSIFICATION/DOWNGRADING SCHEDULE
16. DISTRIBUTION STATEMENT (of this Report) Approved for public release; distribution unlimited.		
17. DISTRIBUTION STATEMENT (of the abstract entered in Block 20, if different from Report)		
18. SUPPLEMENTARY NOTES This Memorandum Report supersedes IMR No. 537 dated January 1977.		
19. KEY WORDS (Continue on reverse side if necessary and identify by block number) M282E1 Shell Angular Momentum T216E1 Shell Moving Internal Shell Parts T306E10 Shell Arming Ball Rotor T317 Shell Internal Projectile Rings M505 Fuze Quasi-linear Angular Motion		
20. ABSTRACT (Continue on reverse side if necessary and identify by block number) (jah) The angular momentum for a projectile with a moving internal part is derived and quasi-linear solutions to the resulting differential equations are obtained. These solutions explain the unusual behavior exhibited by four shells in 1955: M282E1, T216E1, T306E10 and T317.		

DD FORM 1 JAN 73 1473 EDITION OF 1 NOV 65 IS OBSOLETE

UNCLASSIFIED

SECURITY CLASSIFICATION OF THIS PAGE (When Data Entered)

050 750

PRECEDING PAGE MARK

TABLE OF CONTENTS

	Page
LIST OF TABLES	5
LIST OF FIGURES.	7
I. INTRODUCTION	9
II. THEORY	10
III. FAST MODE LOCK-IN.	14
IV. DISCUSSION	15
V. CONCLUSIONS.	18
VI. ACKNOWLEDGMENT	18
REFERENCES	27
LIST OF SYMBOLS.	29
APPENDIX A	37
APPENDIX B	51
APPENDIX C	55
DISTRIBUTION LIST.	57

Preceding page Blank

LIST OF TABLES

<u>Table</u>	<u>Page</u>
1. Parameters for T282E1 at Mach Number 3.3	17
2. Parameters for T317.	19

LIST OF FIGURES

<u>Figure</u>	<u>Page</u>
1. 20mm Shell T282E1 with Arming Ball Rotor.	20
2. Fast Mode Damping Rate for the 20mm T282E1.	21
3. Measured Spin History of the T317	22
4. Simplified Schematic of the T317.	23
5. Computed Angular Motion for the T317 ($\gamma = 0$).	24
6. Computed Spin History for the T317.	25
7. Computed Angular Motion for the T317 ($\gamma = .004$)	26

I. INTRODUCTION

In 1955, four shell types exhibited unusual behavior which involved the movement of their internal parts. Three of these shell - the 20mm M282E1, the 20mm T216E1 and the 30mm T306E10 - showed much less fast mode damping when fired with the M505 fuze¹⁻³. This fuze has a spherical arming rotor in a cylindrical cavity with small but non-zero clearances (Figure 1). The fourth shell - the 8-inch T317 - showed significant range losses and very large spin decays⁴. This shell has several rings held on a central column but free to move with small but non-zero clearances. In all these cases, small amplitude motions of the internal parts had significant effect on the parent shell's motion.

Two types of internal parts motion are possible: (1) linear movements* of their centers of mass relative to the external shell center of mass; (2) angular motion of their spin axes with respect to the external shell spin axis. In order that these internal movements have a significant effect on the shell motion, they must have components at the same frequencies as the shell's pitching and yawing motion. Thus we have an internal resonance situation, but the amplitude of the internal movement is bounded. In this report, we will develop the theory for internal motions that have fixed phase with respect to the angle-of-attack plane and obtain quasi-linear solutions to the resulting differential equations. Next, much simpler results will be obtained for motion which has fixed phase with respect to the plane of the higher frequency component of the pitching and yawing motion. Finally, these results will be used to explain the observed behavior of the four 1955 shell.

*Hodapp⁵ has derived general equations for this motion but applied them to the very simple case of longitudinal motion of a mass on the shell's axis of symmetry.

1. E.D. Boyer, "Comparison of Aerodynamic Characteristics of 20mm HEI Shell M97 with Fuze M75 and 20mm Shell T216E1 with Fuze M505," Ballistic Research Laboratories Memorandum Report 865, April 1955. AD69009.
2. E.D. Boyer, "Aerodynamic Characteristics for Small Yaws of 20mm Shell, HEI, T282E1 with Fuze M505 for Mach Numbers .36 to 3.78," Ballistic Research Laboratories Memorandum Report 916, August 1955. AD77515.
3. E.T. Roecker and E.D. Boyer, "Aerodynamic Characteristics of 30mm HEI Shell, T306E10," Ballistic Research Laboratories Memorandum Report 1098, August 1957. AD152952.
4. B.G. Karpov and J.W. Bradley, "A Study of Causes of Short Ranges of the 8" T317 Shell," Ballistic Research Laboratories Report 1049, May 1958. AD377548.
5. A.E. Hodapp, "Equations of Motion for Constant Mass Entry Vehicles with Time Varying Center of Mass Position," Sandia Laboratories SC-RR-70-691, November 1970.

II. THEORY

The theoretical model consists of two bodies: (1) the external symmetric shell body with mass m_b and (2) the internal rotationally symmetric component with mass m_c . The center of mass of the internal component is allowed to perform a circular motion of radius ϵ normal to the axis of symmetry of the external body maintaining a fixed phase angle, ϕ_ϵ , with the angle of attack plane. The axis of symmetry of the internal component can cant at a small fixed angle, γ , with respect to the axis of symmetry of the external body. The plane of this cant angle is now constrained to rotate about the shell axis, maintaining a constant angle ϕ_γ with the angle-of-attack plane. If θ is the roll orientation angle of the angle-of-attack plane with respect to aeroballistic axes⁶, the polar angle of the circular center of mass motion is

$$\theta_\epsilon = \theta + \phi_\epsilon \quad (1)$$

and the roll angle of the cant plane is

$$\theta_\gamma = \theta + \phi_\gamma \quad (2)$$

In Appendix A, the angular momentum of this two-body system is computed and used to obtain the following differential equations.

$$\begin{aligned} I_{xb} \dot{P}_b + I_{xc} \dot{P}_c &= A_{lp} P_b \\ &- B_\gamma \left[(\dot{\beta} \cos \theta_\gamma + \dot{\alpha} \sin \theta_\gamma) \right]_{av} \gamma \\ &- B_\epsilon \left[(\dot{\beta} \cos \theta_\epsilon + \dot{\alpha} \sin \theta_\epsilon) \dot{\theta} \right]_{av} \epsilon \end{aligned} \quad (3)$$

$$I_t \ddot{\xi} - (A_q + iL_{x0}) \dot{\xi} - (A_\alpha + iA_{p\alpha}) \xi + i(\dot{\Gamma} + \dot{E}) = 0 \quad (4)$$

6. C.H. Murphy, "Free Flight Motion of Symmetric Missiles," Ballistic Research Laboratories Report 1216, July 1963. AD442757.

where

$\tilde{\xi} = \tilde{\beta} + i \tilde{\alpha}$ is the complex angle of attack

I_{xb}, I_{xc} are the roll moments of inertia of masses b and c

I_{tb}, I_{tc} are the pitch moments of inertia of masses b and c

$$B_{\gamma} = I_{xc} p_c - I_{tc} \dot{\theta}$$

$$B_{\epsilon} = m_c x_c \ell$$

$$\Gamma = B_{\gamma} \gamma \exp(i\theta_{\gamma})$$

$$E = B_{\epsilon} \dot{\theta} \epsilon \exp(i\theta_{\epsilon})$$

$$L_{x0} = I_{xb} p_b + I_{xc} p_c$$

and the other symbols are defined in the List of Symbols.

The usual quasi-linear assumption is made that the pitching and yawing motion when the internal motion occurs has the same epicyclic form that describes the rigid body motion:

$$\tilde{\xi} = K_1 e^{i\phi_1} + K_2 e^{i\phi_2} \quad (5)$$

where

$$\dot{K}_j = \lambda_j K_j$$

$$\phi_j = \phi_{j0} + \dot{\phi}_j t$$

In Appendix B, quasi-linear relations for the frequency shifts and damping effects introduced by these internal motions are given.

$$\Delta \dot{\phi}_j = - \dot{\phi}_{jr} K_j^{-1} C_j [2 I_t \dot{\phi}_{jr} - L_{x0}]^{-1} \quad (6)$$

$$\dot{K}_j = \lambda_j K_j + \dot{\phi}_j S_j [2 I_t \dot{\phi}_j - L_{x0}]^{-1} \quad (7)$$

where

$$C_j = [B_{\gamma j} \gamma \cos \phi_\gamma + B_\epsilon \dot{\phi}_j \epsilon \cos \phi_\epsilon] [e^{i\theta}]_j$$

$$S_j = [B_{\gamma j} \gamma \sin \phi_\gamma + B_\epsilon \dot{\phi}_j \epsilon \sin \phi_\epsilon] [e^{i\theta}]_j$$

$$B_{\gamma j} = I_{xc} p_c - I_{tc} \dot{\phi}_j$$

$$[e^{i\theta}]_j = (1/2\pi) \int_0^{2\pi} e^{i(\theta - \phi_j)} d\hat{\phi}$$

$$\hat{\phi} = \phi_2 - \phi_1$$

$$\lambda_j = [A_q \dot{\phi}_j + A_{p\alpha}] [2I_t \dot{\phi}_j - L_{x0}]^{-1}$$

and the $\dot{\phi}_{jr}$ are the frequencies of the rigid body.

The quasi-linear approximations can be inserted in the roll equation (Equation 3) and the result averaged. This is done in Appendix C with the result

$$I_{xb} \dot{p}_b + I_{xc} \dot{p}_c = A_{lp} \dot{p}_b - \dot{\phi}_1 K_{11} S_1 - \dot{\phi}_2 K_{22} S_2 \quad (8)$$

It should be noted⁶ that

$$\dot{\phi}_{1r} + \dot{\phi}_{2r} = L_{x0}/I_t \quad (9)$$

Thus $2I_t \dot{\phi}_j - L_{x0}$ is positive for the fast rate and negative for the slow rate.

Equations (7-8) show that positive S_j 's ($\phi_\epsilon, \phi_\gamma$ in the first or second quadrant) can cause undamping of the fast component (K_1), damping of the slow component (K_2) and a reduction in the spin rate.

Now θ can be determined by the definition

$$e^{i\theta} = \tilde{\xi} \delta^{-1} \quad (10)$$

where

$$\delta = |\tilde{\xi}| = (K_1^2 + K_2^2 + 2K_1 K_2 \cos \hat{\phi})^{1/2}$$

Thus

$$\begin{aligned} [e^{i\theta}]_1 &= \frac{K_1}{2\pi} \int_0^{2\pi} [1 + (K_2/K_1) e^{i\hat{\phi}}] \delta^{-1} d\hat{\phi} \\ &= \frac{K_1}{2\pi} \int_0^{2\pi} [1 + (K_2/K_1) \cos \hat{\phi}] \delta^{-1} d\hat{\phi} \\ &= K_1 [\delta^{-1}]_{e_1} \end{aligned} \quad (11)$$

$$[e^{i\theta}]_2 = K_2 [\delta^{-1}]_{e_2} \quad (12)$$

where⁷

$$[\delta^{-1}]_{e_1} = \frac{1}{\pi K_1^2} [(K_1 - K_2) E_1(k) + (K_1 + K_2) E_2(k)] \quad (13)$$

$$[\delta^{-1}]_{e_2} = \frac{1}{\pi K_2^2} [(K_2 - K_1) E_1(k) + (K_1 + K_2) E_2(k)] \quad (14)$$

$$k^2 = \frac{4K_1 K_2}{(K_1 + K_2)^2}$$

7. C.H. Murphy, "Prediction of the Motion of Missiles Acted on by Non-linear Forces and Moments," Ballistic Research Laboratories Report 995, October 1956. AD122221.

and

E_i is the complete elliptic integral of the i -th kind.

When $K_1 > K_2$, Equations (13-14) can be approximated by

$$[\delta^{-1}]_{e_1} \cong \frac{1 - 0.36(K_2/K_1)^3}{K_1} \quad (15)$$

$$[\delta^{-1}]_{e_2} \cong \frac{0.5 + 0.14(K_2/K_1)^3}{K_1} \quad (16)$$

When $K_2 > K_1$, interchange all 1 and 2 subscripts on both sides of Equations (15-16).

III. FAST MODE LOCK-IN

The preceding section assumed that the ϵ and γ motions had constant phase--that they were "locked-in"--with the angle-of-attack plane. We note from Equations (6-8) that the frequency, damping and roll effect terms for the j -th mode contain $\dot{\phi}_j$ or $\dot{\phi}_j^2$ and thus the effect of the fast mode is much greater than that of the slow mode. This suggests a much simpler theoretical model, namely, one in which the ϵ and γ motions are locked-in with the plane of the fast mode. Then Equation (10) is replaced by

$$\theta = \phi_1 \quad (17)$$

Under this assumption, Equations (4) and (5) very quickly yield

$$\Delta \dot{\phi}_1 = -\dot{\phi}_j r_1^{-1} [B_{\gamma_1} \gamma \cos \phi_\gamma + B_{\epsilon_1} \epsilon \cos \phi_\epsilon] [2I_{t_1} \dot{\phi}_1 - L_{x0}]^{-1} \quad (18)$$

$$\Delta \dot{\phi}_2 = 0 \quad (19)$$

$$\dot{K}_1 = \lambda_{11} K_1 + \dot{\phi}_1 [B_{\gamma_1} \gamma \sin \phi_\gamma + B_{\epsilon_1} \epsilon \sin \phi_\epsilon] [2I_{t_1} \dot{\phi}_1 - L_{x0}]^{-1} \quad (20)$$

$$\dot{K}_2 = \lambda_{22} K_2 \quad (21)$$

Equations (3) and (5) can be combined and averaged to yield

$$I_{xb} \dot{p}_b + I_{xc} \dot{p}_c = A_{\lambda p} p_b - \dot{\phi}_1 K_1 [B_{\gamma 1} \gamma \sin \phi_\gamma + B_{\epsilon 1} \dot{\phi}_1 \epsilon \sin \phi_\epsilon] \quad (22)$$

IV. DISCUSSION

The ball fuze is a case where the center of mass motion can occur but we can assume $\gamma = 0$ and $p_b = p_c$. Equations (20-22) become

$$\dot{K}_1 = \lambda_1 K_1 + \dot{\phi}_1^2 m_c x_c \ell \epsilon \sin \phi_\epsilon [2 I_t \dot{\phi}_1 - I_x p_b]^{-1} \quad (23)$$

$$\dot{K}_2 = \lambda_2 K_2 \quad (24)$$

$$I_x \dot{p}_b = A_{\lambda p} p_b - \dot{\phi}_1^2 K_1 m_c x_c \ell \epsilon \sin \phi_\epsilon \quad (25)$$

In all flights, K_1 remained less than 120 milliradians and no spin-down moment could be observed.

In Figure 2, \dot{K}_1/K_1 is plotted versus Mach number for the 20mm shell T282E1 with and without the ball rotor. For Mach numbers below 2, the exponential damping is well determined, but above this Mach number, considerable scatter occurs. Projectiles whose fuzes did not have the ball rotor have damping rates that lie close to -7 per second while those with the rotor have values that are as much as 9 per second greater (i.e. +2).

This phenomenon for Mach numbers near 2 can be ascribed to the action of a locking spring which releases the ball when the shell spin rate is large enough. For a given twist gun tube and air temperature, the initial spin rate is proportional to the launch Mach number.

The appropriate parameters for the T282E1 at Mach number 3.3 are given in Table 1. For Mach numbers between 2.8 and 3.8, measured K_1 falls between .05 and .12. The observed damping rate discrepancies can be explained by Equation (23) with values of $\lambda \epsilon \sin \phi_e$ between 0.09mm and 0.28 mm. These values are possible for the actual tolerances observed in this shell.

The actual spin histories of several T317's are given in Reference 4 and are repeated as Figure 3. This figure also gives the spin history for three T347. The T347 shell has the same external shape, mass, and moments of inertia but no moveable internal components. In all observed cases, the T317 had a greater spin loss and flew to a lesser range. The relative decrements between the range of each T317 shell and the average range of the T347's is given in the figure. Thus a spin loss of almost 70 Hz was observed for a projectile that flew 11% short of its proper range.

Unfortunately, measurements of angular motion were not made. A range loss of 11% would, however, require an average angular motion amplitude of 10° to 15° . The shell internal construction is fairly complicated but can be theoretically approximated by a single ring freely sliding on a central shaft (Figure 4). The tolerances are quite small but are sufficient to allow the ring to cant at an angle as large as .004 radian. When the ring is fully canted, its center of mass is on the axis of the shell and, hence, ϵ is zero. For simplicity we will assume that the ring is spinning with the shell. The fast mode damping rate as given by Equation (20) becomes:

$$\dot{K}_1 = \lambda_1 K_1 + \dot{\phi}_1 (I_{xc} p_b - I_{tc} \dot{\phi}_1) \gamma \sin \phi_\gamma [2I_{t\dot{\phi}_1} - I_{xp_b}]^{-1} \quad (26)$$

The spin equation (Equation (22)) now reduces to

$$I_{xp_b} \dot{p}_b = A_{\lambda_p} p_b - \dot{\phi}_1 K_1 (I_{xc} p_b - I_{tc} \dot{\phi}_1) \gamma \sin \phi_\gamma \quad (27)$$

For a dynamically stable shell, λ_1 is negative. If ϕ_γ is in the first or second quadrant, the second term in Equation (26) is positive and, hence, K_1 should grow to some equilibrium value. This equilibrium value of K_1 can then be used in Equation (27) to give a spin-down moment. Our theoretical model of the behavior of the T317 is based on the assumption that it has values of A_{λ_p} , γ and ϕ_γ such that its fast mode motion grows to $10-15^\circ$ and causes the observed range loss and spin-down.

TABLE 1. PARAMETERS FOR T282E1 AT MACH NUMBER 3.3

$$\ell = 2.0 \text{ cm}$$

$$C_D = 0.41$$

$$m = 96.6 \text{ gm}$$

$$C_{L_\alpha} = 2.6$$

$$I_x = 53.4 \text{ gm/cm}^2$$

$$C_{M_\alpha} = 2$$

$$I_y = 394 \text{ gm/cm}^2$$

$$C_{M_q} + C_{M_{\dot{\alpha}}} = -5.3$$

$$m_c = 3.0 \text{ gm}$$

$$C_{M_{p\alpha}} = 0.15$$

$$x_c = 2.9 \text{ cm}$$

$$V_o = 1140 \text{ m/s}$$

$$P_o = 1900 \text{ Hz}$$

As a check on this conjecture, Equations (3-4) were coded for a digital computer. Although the complete set of aerodynamic coefficients are not well known for this shell, nominal values were used and are given in Table 2.* Figures 5 and 6 give the yawing motion and spin for the completely rigid shell ($\gamma=0$). The yawing motion shows the usual small amplitude slow mode limit cycle which is frequently observed.

Computer runs were then made for $\gamma = .004$, $\phi_\gamma = 45^\circ$. Figure 7 shows a rapid growth of the fast mode angular motion to about 18° and a decay on the down leg of the trajectory. A range loss of 11% was computed and a large spin-down is shown in Figure 6. The computed spin-down is as large as the observed spin-down but different in detail. Thus we would assume that the actual angular motion grew much slower than our computed motion but reached a much larger maximum value.

In summary then, the theory gives good qualitative agreement with the observed behavior of the T317. In view of the incomplete information on its aerodynamic properties and angular motion, better quantitative results can not be expected.

V. CONCLUSIONS

A theory has been developed for the motion of a projectile with a moving internal component that performs either a forced center of mass motion or a forced precession of its spin axis.

This theory gives a good explanation of the observed reduced damping of shell with a ball rotor in its fuzes and the reduced range and rapid spin-down of a projectile with a ring on a central column.

VI. ACKNOWLEDGMENT

This theoretical work has benefited greatly from discussions with W. Chadwick and W. Soper of Naval Surface Weapons Center/Dahlgren Laboratory, H. Vaughn of Sandia Laboratories, and R. Kline of Picatinny Arsenal. The author is particularly indebted to J. Bradley of BRL for his critical review of the analysis and his programming of the necessary numerical calculations.

**Since a nonlinear Magnus moment was used in the numerical work, Equations (6-7, 26) no longer apply but quasi-linear forms of these equations can be obtained by the usual techniques.⁶*

TABLE 2. PARAMETERS FOR T317

$$I_x/I_t = .1352$$

$$I_{xc}/I_t = .0472$$

$$I_{tc}/I_t = .0251$$

$$C_{D\delta^2} = 3$$

$$C_{\ell p} = -.012$$

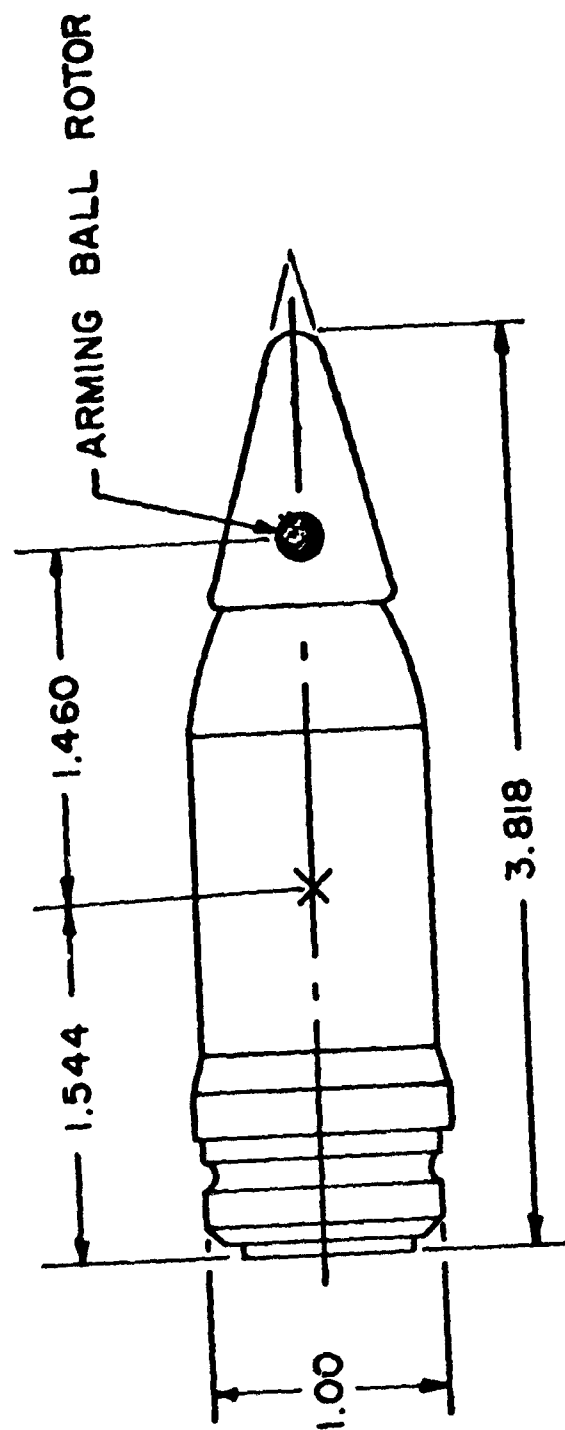
$$C_{L\alpha} = 2.0$$

$$C_{M_q} + C_{M_{\dot{\alpha}}} = -6.3$$

$$C_D = \begin{cases} .218 & M < .88 \\ -.9612 + 1.34M & .88 \leq M \leq 1.1 \\ .6503 - .125M & M > 1.1 \end{cases}$$

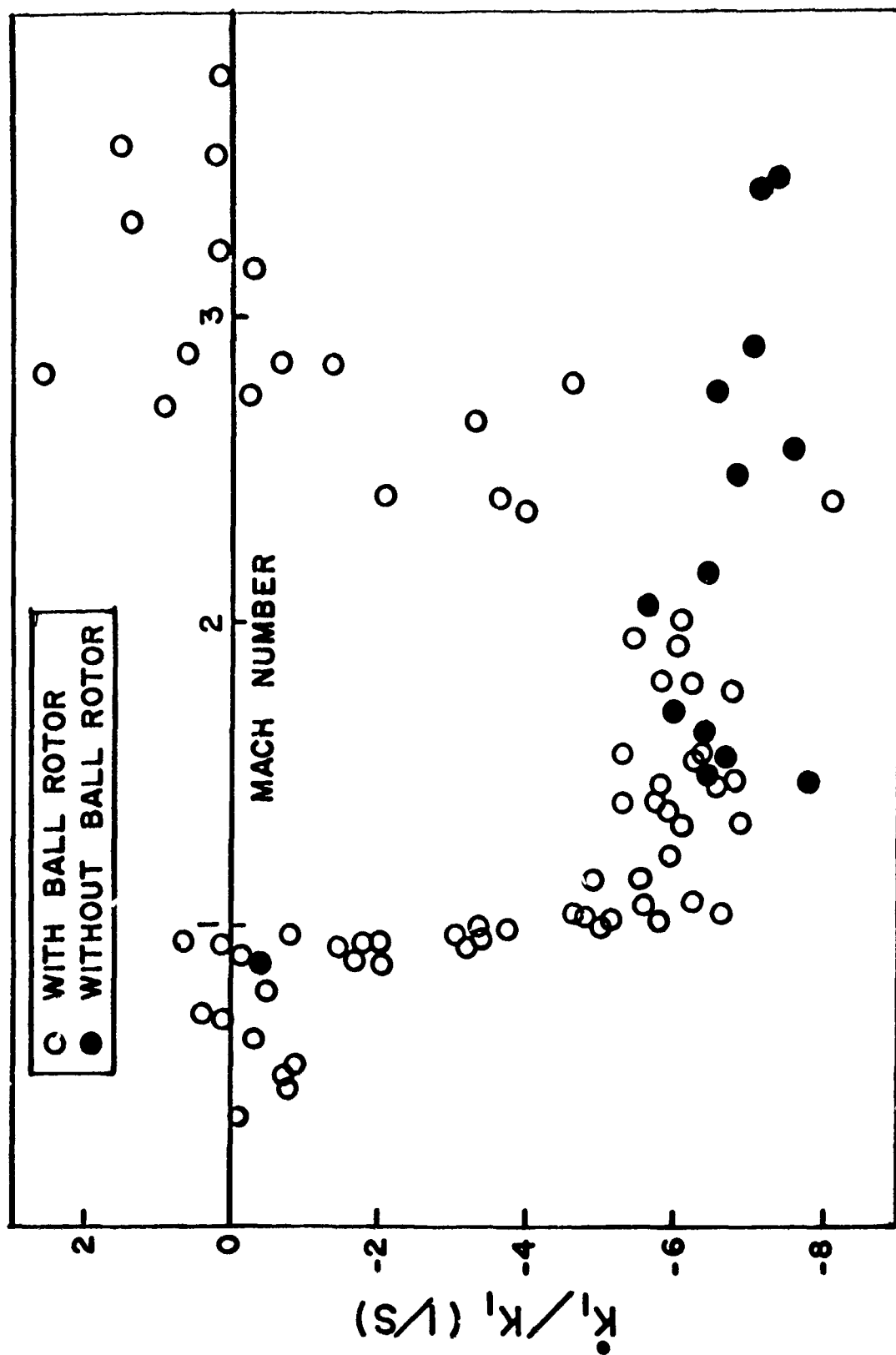
$$C_{M_\alpha} = \begin{cases} 4.4 & M < .88 \\ 1.32 + 3.5M & .88 \leq M \leq 1.1 \\ 5.17 & M > 1.1 \end{cases}$$

$$C_{M_{p\alpha}} = \begin{cases} -.26 + 9\delta^2 & \delta \leq 0.1 \\ -.017 \delta^{-1} & \delta > 0.1 \end{cases}$$



(ALL DIMENSIONS IN CALIBRES)

Figure 1. 20mm She11 T282E1 with Arming Ball Rotor



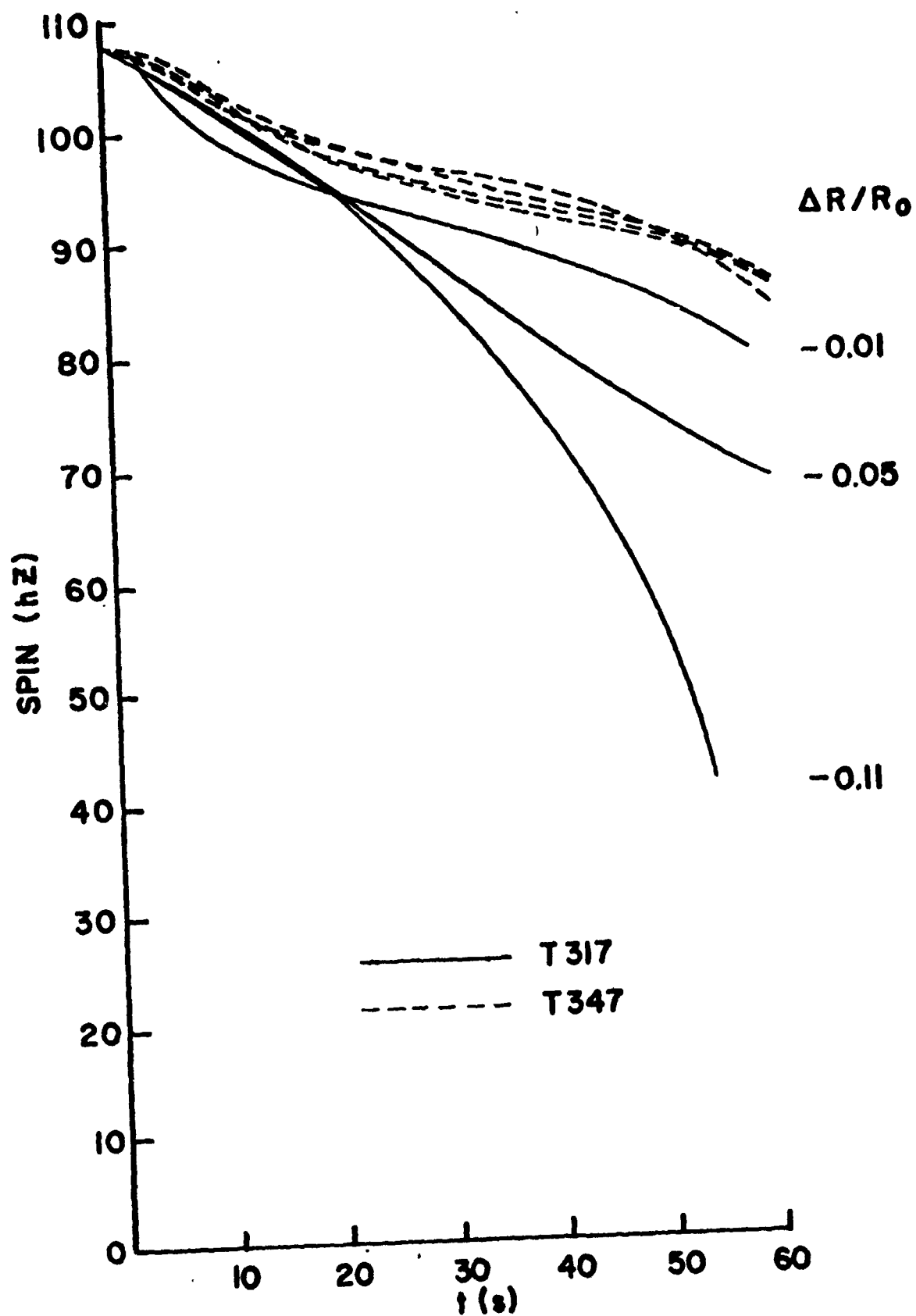


Figure 3. Measured Spin History of the T317

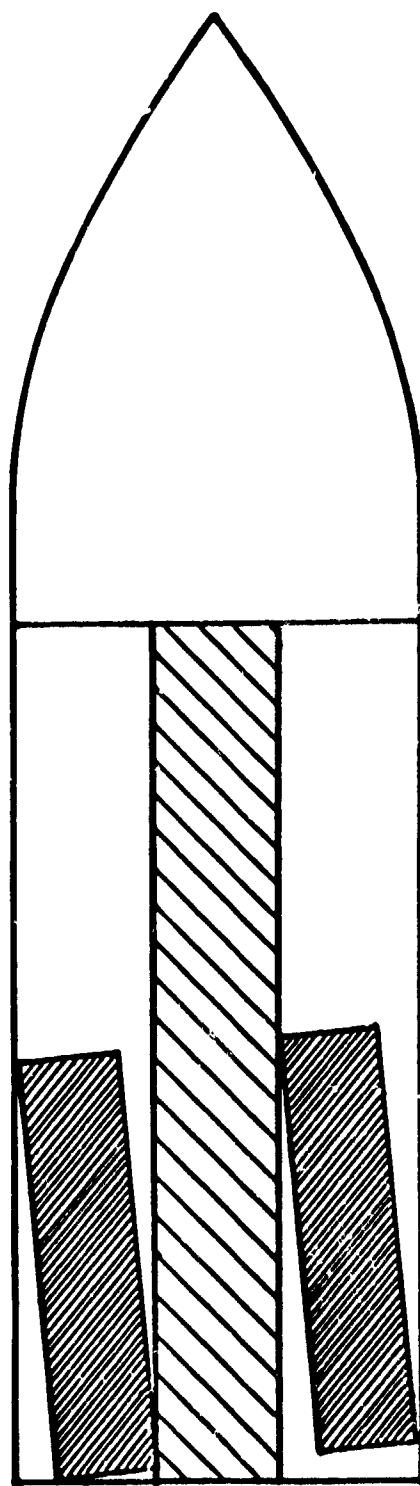


Figure 4. Simplified Schematic of the T317

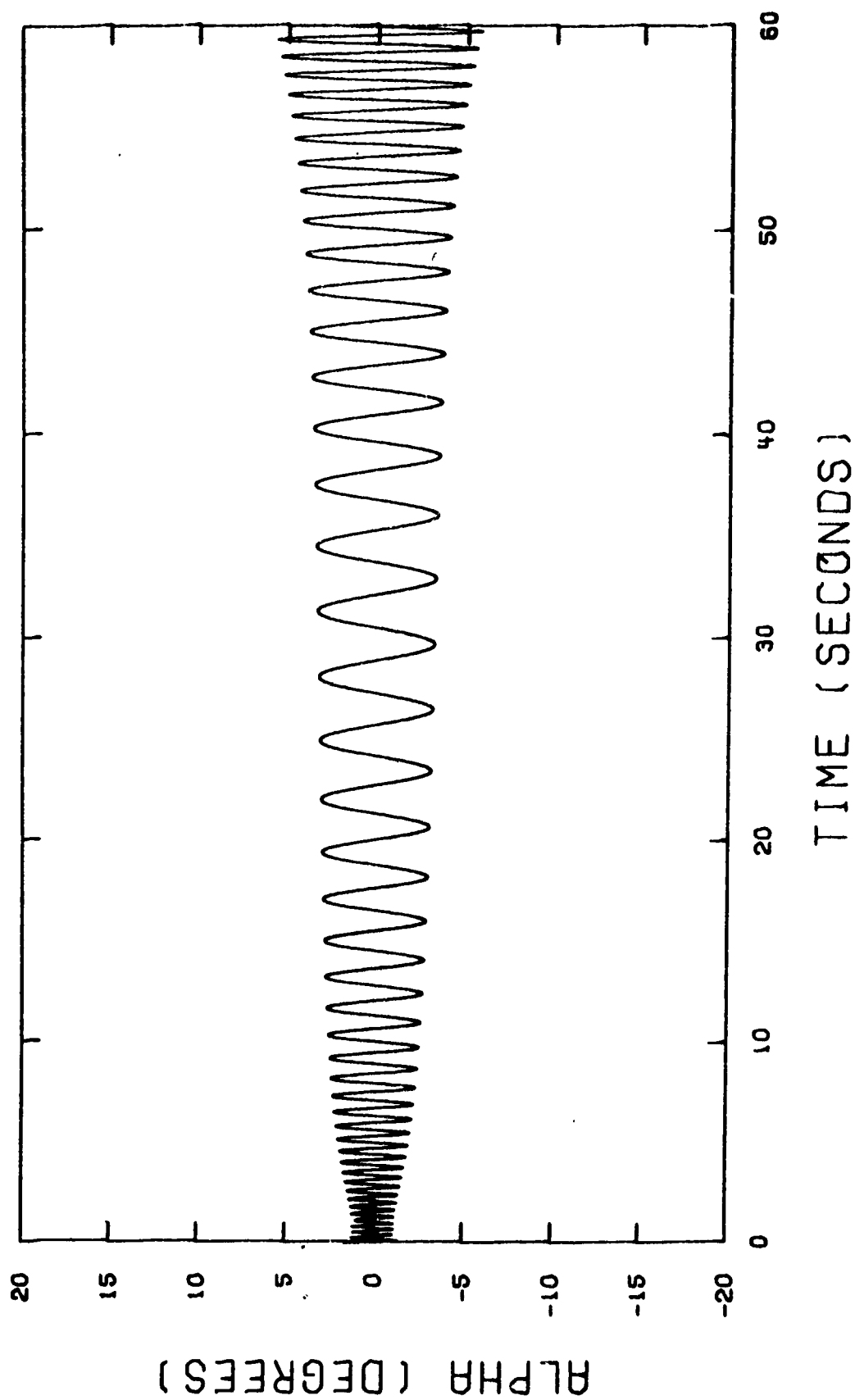


Figure 5. Computed Angular Motion for the T317 ($\gamma = 0$)

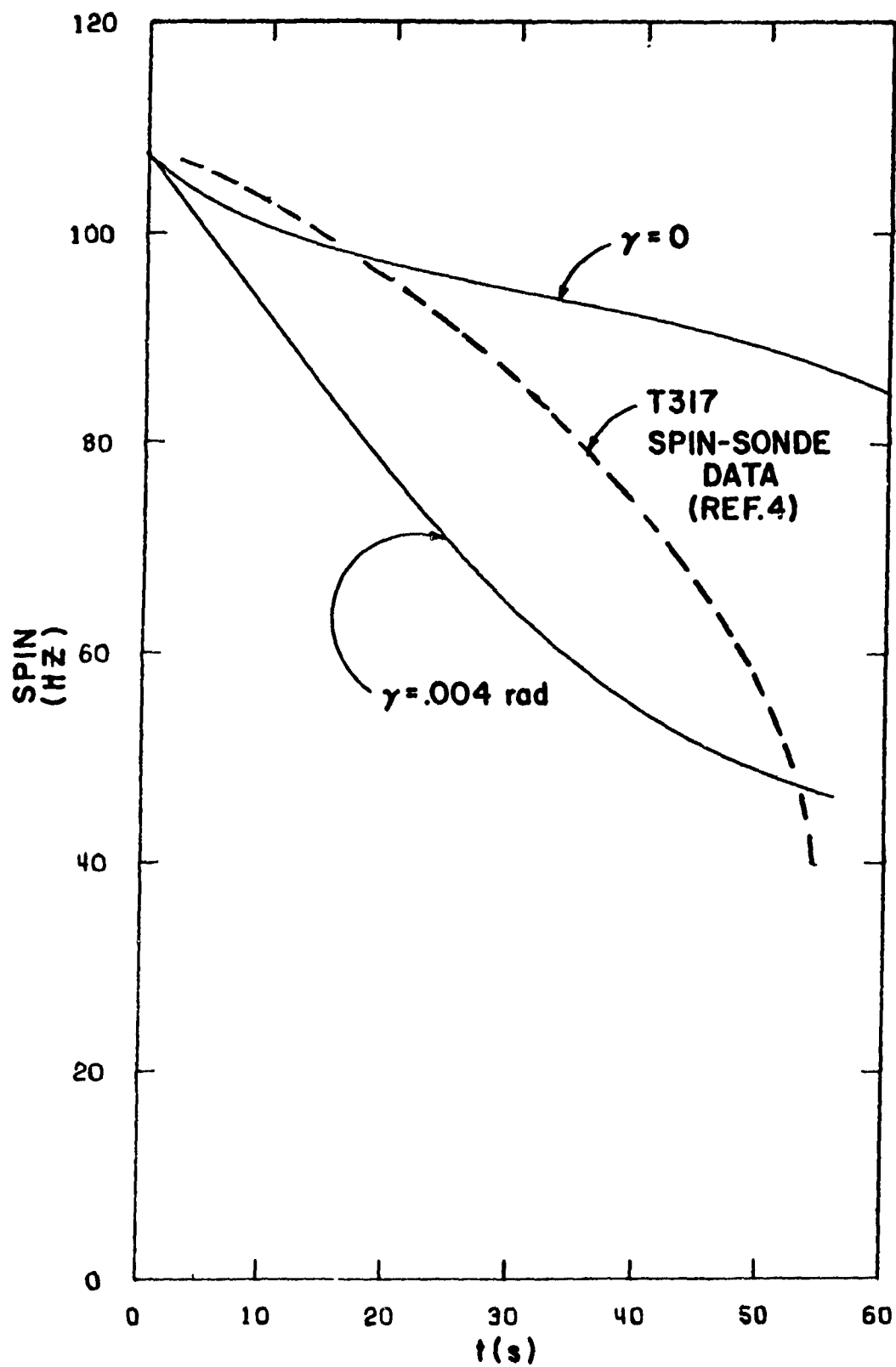


Figure 6. Computed Spin History for the T317

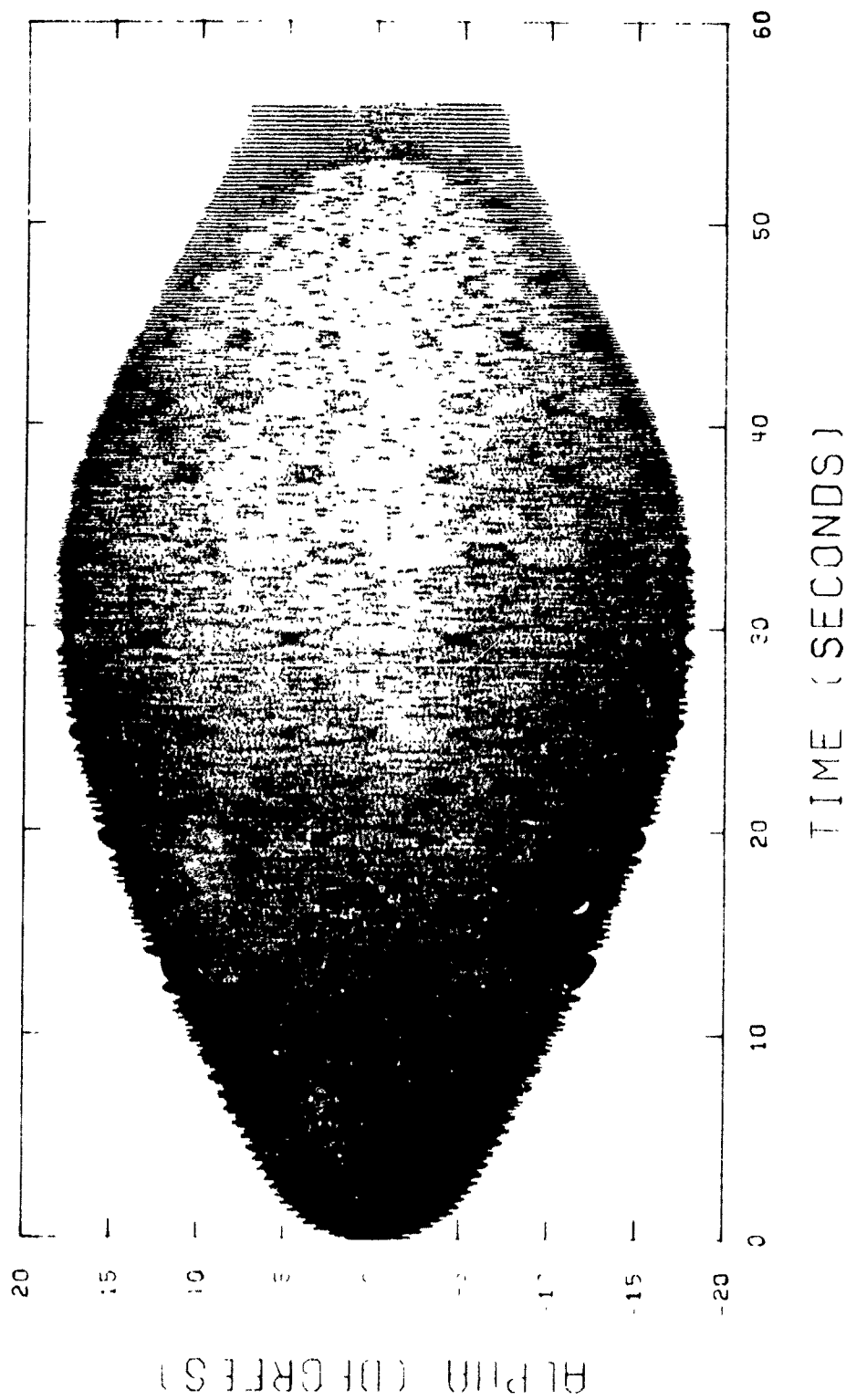


Figure 7. Computed Angular Motion for the T317 ($\gamma = .004$)

REFERENCES

1. E. D. Boyer, "Comparison of Aerodynamic Characteristics of 20mm HEI Shell M97 with Fuze M75 and 20mm Shell T216E1 with Fuze M505," U.S. Army Ballistic Research Laboratories Memorandum Report No. 865, April 1955, AD 69009.
2. E. D. Boyer, "Aerodynamic Characteristics for Small Yaws of 20mm Shell, HEI, T282E1 with Fuze M505 for Mach Numbers .36 to 3.78," U.S. Army Ballistic Research Laboratories Memorandum Report No. 916, August 1955, AD 77515.
3. E. T. Roecker and E. D. Boyer, "Aerodynamic Characteristics of 30mm HEI Shell, T306E10," U.S. Army Ballistic Research Laboratories Memorandum Report No. 1098, August 1957, AD 152952.
4. B. G. Karpov and J. W. Bradley, "A Study of Causes of Short Ranges of the 8" T317 Shell," U.S. Army Ballistic Research Laboratories Report No. 1049, May 1958, AD 377548.
5. A. E. Hodapp, "Equations of Motion for Constant Mass Entry Vehicles with Time Varying Center of Mass Position," Sandia Laboratories SC-RR-70-691, November 1970.
6. C. H. Murphy, "Free Flight Motion of Symmetric Missiles," U.S. Army Ballistic Research Laboratories Report No. 1216, July 1963, AD 442757.
7. C. H. Murphy, "Prediction of the Motion of Missiles Acted on by Non-Linear Forces and Moments," U.S. Army Ballistic Research Laboratories Report No. 995, October 1956, AD 122221.
8. Herbert Goldstein, Classical Mechanics, Reading, Massachusetts, Addison-Wesley Publishing Company, Inc., 1950.

LIST OF SYMBOLS*

$A_{\ell p}$	$(1/2)\rho S\ell^2VC_{\ell p}$
$A_{p\alpha}$	$(1/2)\rho S\ell^2V[p_b C_{M_{p\alpha}} + (L_{x0}/m\ell^2) C_{L_\alpha}]$
A_q	$(1/2)\rho S\ell^2V[C_{M_q} + C_{M_\alpha} - (I_t/m\ell^2) C_{L_\alpha}]$
A_α	$(1/2)\rho S\ell V^2 C_{M_\alpha}$
B_γ	$I_{xc} \dot{p}_c - I_{tc} \dot{\theta}$
$B_{\gamma j}$	$I_{xc} \dot{p}_c - I_{tc} \dot{\phi}_j, j = 1, 2$
B_ϵ	$m_c x_c \ell$
C_j	$(B_{\gamma j} \gamma \cos \phi_\gamma + B_\epsilon \dot{\phi}_j \epsilon \cos \phi_\epsilon) [e^{i\theta}]_j, j = 1, 2$
$C_{\ell p}$	roll damping moment coefficient, Equation (A39)
C_{L_α}	lift force coefficient, Equation (A41)
$C_{M_{p\alpha}}$	Magnus moment coefficient, Equation (A40)
C_{M_q}, C_{M_α}	damping moment coefficients, Equation (A40)
C_{M_α}	static moment coefficient, Equation (A40)

*In this List, the words "projectile," "body" and "internal component" are used in the sense that the projectile consists of an external symmetric body and an internal symmetric component.

LIST OF SYMBOLS (Continued)

$\vec{e}_1, \vec{e}_2, \vec{e}_3$	unit vectors in the nonrolling aeroballistic system, \vec{e}_1 along the body's axis of symmetry
$\vec{e}_{1c}, \vec{e}_{2c}, \vec{e}_{3c}$	unit vectors in the internal component's coordinate system, \vec{e}_{1c} along the internal component's axis of symmetry and \vec{e}_{3c} normal to \vec{e}_1 , Equations (A23-A25)
$[e^{i\theta}]_j$	$\frac{1}{2\pi} \int_0^{2\pi} e^{i(\theta-\phi_j)} d\phi, j = 1,2$
$E_i(k)$	complete elliptic integral of the i-th kind, $i = 1,2$, with modulus k
I_x, I_t	axial and transverse moments of inertia of the projectile
I_{xb}, I_{tb}	axial and transverse moments of inertia of the body, Equation (A20)
I_{xc}, I_{tc}	axial and transverse moments of inertia of the internal component, Equation (A31)
K_j	length of the j-th modal arm, $j = 1,2$
ℓ	reference length
\vec{L}	angular momentum vector of the projectile
\vec{L}_b, \vec{L}_c	angular momentum vector of the body and internal component, respectively
L_{x0}	$I_{xb} p_b + I_{xc} p_c$
m	the mass of the projectile, $m_b + m_c$
m_b	mass of the body

LIST OF SYMBOLS (Continued)

m_c	mass of the internal component
M_x, M_y, M_z	components of the aerodynamic moment vector in the nonrolling aeroballistic system, Equations (A39-A40)
p, q, r	components of the projectile's angular velocity in the missile-fixed coordinate system, Equation (A1)
$\tilde{p}, \tilde{q}, \tilde{r}$	components of the projectile's angular velocity in the nonrolling aeroballistic system, Equation (A4)
p_b	$\dot{\phi}_b$, the roll rate of the body
p_c	$\dot{\phi}_c + \dot{\theta}$, the roll rate of the internal component
Q	$\tilde{q} + i\tilde{r}$
\hat{r}_b	distance of the body submass dm from the \vec{e}_1 -axis, Equation (A12)
\vec{r}_b	vector from the center of mass of the projectile to the center of mass of the body, Equation (A8)
\vec{R}_b	vector from the center of mass of the body to the submass dm of the body, Equation (A12)
\hat{r}_c	distance of the internal component submass dm from the \vec{e}_{1c} -axis, Equation (A29)
\vec{r}_c	vector from the center of mass of the projectile to the center of mass of the internal component, Equation (A9)

LIST OF SYMBOLS (Continued)

\vec{R}_c	vector from the center of mass of the internal component to the submass dm of the component, Equation (A29)
S	reference area
S_j	$(B_{Yj} \gamma \sin \phi_Y + B_{\epsilon j} \dot{\phi}_\epsilon \sin \phi_\epsilon) [e^{i\theta}]_j, j = 1, 2$
t	time
V	magnitude of the velocity vector
x, y, z	missile-fixed coordinates, with the x-axis along the body's axis of symmetry, the y-axis initially pointed down and rolling with the body and the z-axis determined by the right-hand rule
x_b, \hat{x}_b, x_c	\vec{e}_1 -component of \vec{r}_b, \vec{R}_b and \vec{r}_c , respectively
\hat{x}_c	\vec{e}_{1c} -component of \vec{R}_c
$\tilde{\alpha}, \tilde{\beta}$	angles of attack and sideslip in the nonrolling aeroballistic system
γ	the cant angle: the angle (assumed small and constant) between the axis of symmetry of the internal component and the axis of symmetry of the body
Γ	$B_Y \gamma \exp(i\theta_Y)$
δ	$ \tilde{\xi} $

LIST OF SYMBOLS (Continued)

$[\delta^{-1}]_{ej}$	$\frac{1}{\pi K_j^2} [(K_j - K_{3-j})E_1(k) + (K_1 + K_2)E_2(k)], j = 1, 2$
$\Delta \dot{\phi}_j$	$\dot{\phi}_j - \dot{\phi}_{jr}, j = 1, 2$
ϵ	$\epsilon_b + \epsilon_c$, the nondimensional radius of the circular motion performed by the center of mass of the internal component about the axis of symmetry of the body
ϵ_b	$(\frac{m_c}{m})\epsilon$
ϵ_c	$(\frac{m_b}{m})\epsilon$
E	$B_\epsilon \dot{\theta} \epsilon \exp(i\theta_\epsilon)$
θ	the orientation angle of the angle-of-attack plane with respect to the aeroballistic axes ($\delta e^{i\theta} = \tilde{\xi}$); in most relations, θ can be approximated by ϕ_1
θ_γ	the orientation angle of the cant plane with respect to the aeroballistic axes
θ_ϵ	the polar angle of the circular motion performed by the center of mass of the internal component about the axis of symmetry of the body
λ_j	$(A_q \dot{\phi}_j + A_{p\alpha}) / (2I_t \dot{\phi}_j - L_{x0})$, the j-th damping rate (\dot{K}_j / K_j) for a rigid projectile, $j = 1, 2$
$\tilde{\xi}$	$\tilde{\beta} + i\tilde{\alpha}$, the complex angle of attack
ρ	air density

LIST OF SYMBOLS (Continued)

ϕ_b	the polar angle in the $\vec{e}_2 - \vec{e}_3$ plane of the body submass, Equation (A12)
ϕ_c	the polar angle in the $\vec{e}_{2c} - \vec{e}_{3c}$ plane of the internal component submass, Equation (A29)
ϕ_j	$\phi_{j0} + \dot{\phi}_j t$, the orientation angle of the j-th modal arm, $j = 1, 2$
ϕ_{j0}	initial orientation angle of the j-th modal arm, $j = 1, 2$
$\dot{\phi}_j$	frequency of the j-th modal arm, $j = 1, 2$ (it is assumed that $\dot{\phi}_1 > \dot{\phi}_2$, that is, the 1-arm is the fast arm)
$\dot{\phi}_{jr}$	frequency of the j-th modal arm for a rigid projectile, $j = 1, 2$
ϕ_Y	$\theta_Y - \theta$, assumed constant
ϕ_E	$\theta_E - \theta$, assumed constant
$\hat{\phi}$	$\phi_2 - \phi_1$
$\vec{\omega}$	angular velocity of the projectile, Equations (A1, A4)
$\vec{\Omega}_{mf}$	angular velocity of the missile-fixed coordinate system, Equations (A2, A4)
$\vec{\Omega}$	angular velocity of the nonrolling aeroballistic coordinate system, Equations (A3, A5)

LIST OF SYMBOLS (Continued)

Subscripts

$$[]_{av} \quad \frac{1}{2\pi} \int_0^{2\pi} [] d\hat{\phi}$$

b,c body, internal component

x, \tilde{y} , \tilde{z} vector components in the nonrolling aeroballistic system

Special Notation

a + ib complex representation of the vector $a\vec{e}_2 + b\vec{e}_3$

($\dot{}$) d()/dt

APPENDIX A. DERIVATION OF EQUATIONS OF MOTION

A missile-fixed coordinate system can be defined with x-axis along the missile axis of symmetry, z-axis initially pointed down and rolling with the missile, and a y-axis determined by the right-hand rule. If the angular velocity of the missile in these coordinates is

$$\vec{\omega} = (p, q, r) \quad (A1)$$

the angular velocity of the coordinate system is

$$\vec{\Omega}_{mf} = (p, q, r) \quad (A2)$$

For the motion of symmetric missiles, a much more convenient coordinate system is the aeroballistic system, which pitches and yaws with the missile but has zero roll rate. Its angular velocity vector in missile-fixed coordinates is

$$\vec{\Omega} = (0, q, r) \quad (A3)$$

Transverse components of a vector in the nonrolling coordinates will be identified by tilde superscripts. In aeroballistic coordinates, the three angular velocity vectors assume the form

$$\vec{\omega} = \vec{\Omega}_{mf} = p \vec{e}_1 + \tilde{q} \vec{e}_2 + \tilde{r} \vec{e}_3 \quad (A4)$$

$$\vec{\Omega} = \tilde{q} \vec{e}_2 + \tilde{r} \vec{e}_3 \quad (A5)$$

where $\vec{e}_1, \vec{e}_2, \vec{e}_3$ are unit vectors along the aeroballistic axes.

We now consider the projectile to consist of its external symmetric body with mass m_b and an internal symmetric component of mass m_c which is free to move perpendicular to the body's axis of symmetry. The axis of symmetry of the internal mass is assumed to cant at constant angle γ with respect to the body's axis of symmetry and the plane of this cant angle is assumed to maintain a constant phase angle ϕ_γ with the angle-of-attack plane. If θ and θ_γ are the

orientation angles of the angle-of-attack plane and the cant plane, respectively, then

$$\theta_Y = \theta + \phi_Y \quad (A6)$$

The motion of the center of mass of the internal component will be assumed to be a circular motion of amplitude $\ell\epsilon$ and constant phase angle ϕ_ϵ with respect to the angle-of-attack plane. If θ_ϵ is the phase angle of this center of mass motion, then

$$\theta_\epsilon = \theta + \phi_\epsilon \quad (A7)$$

With respect to the body-plus-internal-component center of mass, both the body and the component are performing circular motions with radii $\ell\epsilon_b$ and $\ell\epsilon_c$, respectively. The vectors locating these two centers of mass with respect to the projectile center of mass are

$$\vec{r}_b = x_b \vec{e}_1 + \ell\epsilon_b (\vec{e}_2 \cos \theta_\epsilon + \vec{e}_3 \sin \theta_\epsilon) \quad (A8)$$

$$\vec{r}_c = x_c \vec{e}_1 - \ell\epsilon_c (\vec{e}_2 \cos \theta_\epsilon + \vec{e}_3 \sin \theta_\epsilon) \quad (A9)$$

$$x_b m_b + x_c m_c = 0 \quad (A10)$$

where

$$\epsilon_b = m_c \epsilon / m$$

$$\epsilon_c = m_b \epsilon / m$$

$$m = m_b + m_c$$

The angular momentum vector of the body, \vec{L}_b , can now be computed from its definition⁸ in terms of a large number of small submasses,

8. Herbert Goldstein, *Classical Mechanics*, Reading, Massachusetts, Addison-Wesley Publishing Company, Inc., 1950.

dm, with position vectors $\vec{r}_b + \vec{R}_b$.

$$\begin{aligned}\vec{L}_b &= \int (\vec{r}_b + \vec{R}_b) \times (\dot{\vec{r}}_b + \dot{\vec{R}}_b) dm \\ &= m_b \vec{r}_b \times \dot{\vec{r}}_b + \int (\vec{R}_b \times \dot{\vec{R}}_b) dm\end{aligned}\quad (A11)$$

The rotational symmetry of the body can be best exploited by expressing the position vectors of the submasses in cylindrical coordinates:

$$\vec{R}_b = \hat{x}_b \vec{e}_1 + \hat{r}_b [\vec{e}_2 \cos \phi_b + \vec{e}_3 \sin \phi_b] \quad (A12)$$

The rotational symmetry implies several useful integral relationships:

$$\int \hat{x}_b \hat{r}_b \cos \phi_b dm = \int \hat{x}_b \hat{r}_b \sin \phi_b dm = 0 \quad (A13)$$

$$\int \hat{r}_b^2 \sin \phi_b \cos \phi_b dm = 0 \quad (A14)$$

$$\int \hat{r}_b^2 \cos^2 \phi_b dm = \int \hat{r}_b^2 \sin^2 \phi_b dm = (1/2) \int \hat{r}_b^2 dm \quad (A15)$$

Since the body is spinning with respect to the aeroballistic axes, it should be emphasized that $\dot{\phi}_b$ is not zero. The derivatives of \vec{r}_b and \vec{R}_b can, however, be easily computed using the relation

$$\dot{\vec{e}}_j = \vec{\Omega} \times \vec{e}_j \quad (A16)$$

$$\therefore \dot{\vec{r}}_b = - \ell \epsilon_b \dot{\theta} (\vec{e}_2 \sin \theta_\epsilon - \vec{e}_3 \cos \theta_\epsilon) + \vec{\Omega} \times \vec{r}_b \quad (A17)$$

$$\dot{\vec{R}}_b = - \hat{r}_b \dot{\phi}_b (\vec{e}_2 \sin \phi_p - \vec{e}_3 \cos \phi_p) + \vec{\Omega} \times \vec{R}_b \quad (A18)$$

The first cross product in the angular momentum equation (Equation (A11)) can now be computed from Equations (A8) and (A17) and simplified by neglecting terms involving ϵ_b^2 .

$$\begin{aligned} \vec{r}_b \times \dot{\vec{r}}_b &= - x_b \ell \epsilon_b \dot{\theta} (\vec{e}_2 \cos \theta_\epsilon + \vec{e}_3 \sin \theta_\epsilon) \\ &\quad + \vec{r}_b \times (\vec{\Omega} \times \vec{r}_b) \\ &= - x_b \ell \epsilon_b (\tilde{q} \cos \theta_\epsilon + \tilde{r} \sin \theta_\epsilon) \vec{e}_1^* \\ &\quad + (\tilde{q} x_b^2 - x_b \ell \epsilon_b \dot{\theta} \cos \theta_\epsilon) \vec{e}_2 \\ &\quad + (\tilde{r} x_b^2 - x_b \ell \epsilon_b \dot{\theta} \sin \theta_\epsilon) \vec{e}_3 \end{aligned} \quad (A19)$$

The integral in Equation (A11) can be simplified quite easily to a familiar form. This is due to the fact that the aeroballistic axes are normal axes of inertia for the body.

$$\begin{aligned} \int (\vec{R}_b \times \dot{\vec{R}}_b) dm &= \dot{\phi}_b I_{xb} \vec{e}_1 + \int \vec{R}_b \times (\vec{\Omega} \times \vec{R}_b) dm \\ &= \dot{\phi}_b I_{xb} \vec{e}_1 + I_{tb} (\tilde{q} \vec{e}_2 + \tilde{r} \vec{e}_3) \end{aligned} \quad (A20)$$

where

$$I_{xb} = \int \hat{r}_b^2 dm$$

$$I_{tb} = \int (\hat{x}_b^2 + (1/2) \hat{r}_b^2) dm$$

Equations (A19-A20) can now be used to compute the angular momentum of the body from Equation (A11):

$$\vec{L}_b = L_{xb} \vec{e}_1 + L_{yb} \vec{e}_2 + L_{zb} \vec{e}_3 \quad (A21)$$

where

$$L_{xb} = p_b I_{xb} + B_\epsilon \epsilon_b (\tilde{q} \cos \theta_\epsilon + \tilde{r} \sin \theta_\epsilon)$$

$$L_{yb} = \tilde{q} (I_{tb} + m_b x_b^2) + B_\epsilon \epsilon_b \dot{\theta} \cos \theta_\epsilon$$

$$L_{zb} = \tilde{r} (I_{tb} + m_b x_b^2) + B_\epsilon \epsilon_b \dot{\theta} \sin \theta_\epsilon$$

$$p_b = \dot{\phi}_b ; \quad B_\epsilon = m_c x_c \ell$$

The angular momentum of the internal component can be computed in a similar way

$$\vec{L}_c = m_c \vec{r}_c \times \dot{\vec{r}}_c + \int \vec{R}_c \times \dot{\vec{R}}_c dm \quad (A22)$$

The integral in Equation (A22) can best be treated by the introduction of axes that pitch and yaw with the internal component. These axes can be selected so that they are normal axes of inertia for the internal component. For small cant angles ($\gamma < 0.1$), unit vectors along these axes can be defined by the following equations:

$$\vec{e}_{1c} = \vec{e}_1 + \gamma [\vec{e}_2 \cos \theta_\gamma + \vec{e}_3 \sin \theta_\gamma] \quad (A23)$$

$$\vec{e}_{2c} = -\gamma \vec{e}_1 + \vec{e}_2 \cos \theta_\gamma + \vec{e}_3 \sin \theta_\gamma \quad (A24)$$

$$\vec{e}_{3c} = -\vec{e}_2 \sin \theta_\gamma + \vec{e}_3 \cos \theta_\gamma \quad (A25)$$

The derivatives of these unit vectors can be computed in terms of $\dot{\theta}$ and the derivatives of the aeroballistic unit vectors.

$$\dot{\vec{e}}_{1c} = -\dot{\theta}_\gamma [\vec{e}_2 \sin \theta_\gamma - \vec{e}_3 \cos \theta_\gamma] + \vec{\Omega} \times \vec{e}_{1c} \quad (A26)$$

$$\dot{\vec{e}}_{2c} = -\dot{\theta} [\vec{e}_2 \sin \theta_\gamma - \vec{e}_3 \cos \theta_\gamma] + \vec{\Omega} \times \vec{e}_{2c} \quad (A27)$$

$$\dot{\vec{e}}_{3c} = -\dot{\theta} [\vec{e}_2 \cos \theta_\gamma + \vec{e}_3 \sin \theta_\gamma] + \vec{\Omega} \times \vec{e}_{3c} \quad (A28)$$

The position vector of the internal component's submasses can now be given in cylindrical coordinates and the \vec{e}_{jc} unit vectors.

$$\vec{R}_c = \hat{x}_c \vec{e}_{1c} + \hat{r}_c [\vec{e}_{2c} \cos \phi_c + \vec{e}_{3c} \sin \phi_c] \quad (A29)$$

The derivative of this vector is somewhat more complicated than the derivative of \vec{R}_b since a term involving the precession rate, $\dot{\theta}$, is present.

$$\begin{aligned}\dot{\vec{R}}_c = & - \hat{r}_c \dot{\phi}_c (\vec{e}_{2c} \sin \phi_c - \vec{e}_{3c} \cos \phi_c) \\ & - \dot{\theta} \left\{ [\gamma \hat{x}_c \sin \theta_\gamma + \hat{r}_c \sin (\phi_c + \theta_\gamma)] \vec{e}_2 \right. \\ & \left. - [\gamma \hat{x}_c \cos \theta_\gamma + \hat{r}_c \cos (\phi_c + \theta_\gamma)] \vec{e}_3 \right\} \\ & + \vec{\Omega} \times \vec{R}_c\end{aligned}\tag{A30}$$

The integral in Equation (A22) can now be computed in a similar fashion as was done for the integral in Equation (A11) since symmetry conditions like Equations (A13-A15) apply. An additional term involving the precession rate, $\dot{\theta}$, must, of course, appear.

$$\begin{aligned}\int \vec{R}_c \times \dot{\vec{R}}_c \, dm = & \dot{\phi}_c I_{xc} \vec{e}_{1c} \\ & + \dot{\theta} [I_{xc} \vec{e}_1 + \gamma (I_{xc} - I_{tc}) (\vec{e}_2 \cos \theta_\gamma + \vec{e}_3 \sin \theta_\gamma)] \\ & + \int \vec{R}_c \times (\vec{\Omega} \times \vec{R}_c) \, dm\end{aligned}\tag{A31}$$

where

$$I_{xc} = \int \hat{r}_c^2 dm$$

$$I_{tc} = \int [\hat{x}_c^2 + (1/2) \hat{r}_c^2] dm$$

The integral on the left side of Equation (A31) can easily be handled if the unit vectors along the normal axes of inertia of the internal component are used.

$$\begin{aligned} \int \vec{R}_c \times (\vec{\Omega} \times \vec{R}_c) dm &= \Omega_{1c} I_{xc} \vec{e}_{1c} + I_{tc} (\Omega_{2c} \vec{e}_{2c} + \Omega_{3c} \vec{e}_{3c}) \\ &= (I_{xc} - I_{tc}) \Omega_{1c} \vec{e}_{1c} + I_{tc} \vec{\Omega} \end{aligned} \quad (A32)$$

where

$$\Omega_{jc} = \vec{\Omega} \cdot \vec{e}_{jc}$$

Since the first cross-product in Equation (A22) can be handled by an equation similar to Equation (A19), Equations (A31-A32) can be used to yield the angular momentum of the internal component in the aeroballistic axes.

$$\vec{L}_c = L_{xc} \vec{e}_1 + L_{yc} \vec{e}_2 + L_{zc} \vec{e}_3 \quad (A33)$$

where

$$L_{xc} = I_{xc} p_c + (I_{xc} - I_{tc}) \gamma (\tilde{q} \cos \theta_\gamma + \tilde{r} \sin \theta_\gamma) \\ + B_\epsilon \epsilon_c (\tilde{q} \cos \theta_\epsilon + \tilde{r} \sin \theta_\epsilon)$$

$$L_{yc} = (I_{tc} + m_c x_c^2) \tilde{q} + B_\gamma \gamma \cos \theta_\gamma \\ + B_\epsilon \dot{\theta} \epsilon_c \cos \theta_\epsilon$$

$$L_{zc} = (I_{tc} + m_c x_c^2) \tilde{r} + B_\gamma \gamma \sin \theta_\gamma \\ + B_\epsilon \dot{\theta} \epsilon_c \sin \theta_\epsilon$$

$$p_c = \dot{\phi}_c + \dot{\theta} \quad ; \quad B_\gamma = I_{xc} p_c - I_{tc} \dot{\theta}$$

Equations (A21) and (A33) can be added to yield the total angular momentum of the projectile:

$$\vec{L} = L_x \vec{e}_1 + L_y \vec{e}_2 + L_z \vec{e}_3 \quad (A34)$$

where

$$L_x = L_{x0} + (I_{xc} - I_{tc}) \gamma (\tilde{q} \cos \theta_\gamma + \tilde{r} \sin \theta_\gamma)$$

$$+ B_\epsilon \epsilon (\tilde{q} \cos \theta_\epsilon + \tilde{r} \sin \theta_\epsilon)$$

$$\dot{L}_y = I_t \dot{\tilde{q}} + B_\gamma \gamma \cos \theta_\gamma + B_\epsilon \dot{\theta} \epsilon \cos \theta_\epsilon$$

$$\dot{L}_z = I_t \dot{\tilde{r}} + B_\gamma \gamma \sin \theta_\gamma + B_\epsilon \dot{\theta} \epsilon \sin \theta_\epsilon$$

$$L_{x0} = I_{xb} p_b + I_{xc} p_c$$

$$I_t = I_{tb} + I_{tc} + m_b x_b^2 + m_c x_c^2$$

The differential equations for the angular motion can now be computed in the usual way.

$$\dot{\vec{L}} = \dot{L}_x \vec{e}_1 + \dot{L}_y \vec{e}_2 + \dot{L}_z \vec{e}_3 + \vec{\Omega} \times \vec{L}$$

$$= M_x \vec{e}_1 + M_y \vec{e}_2 + M_z \vec{e}_3 \quad (A35)$$

The roll equation is obtained from the first component of Equation (A35):

$$\begin{aligned} \dot{L}_x + B_\gamma (\tilde{q} \sin \theta_\gamma - \tilde{r} \cos \theta_\gamma) \gamma \\ + B_\epsilon \dot{\theta} (\tilde{q} \sin \theta_\epsilon - \tilde{r} \cos \theta_\epsilon) \epsilon = M_x \end{aligned} \quad (A36)$$

Since our primary interest in the rolling motion is in its average behavior, \dot{L}_x can be replaced by its average.

$$(\dot{L}_x)_{av} = \dot{L}_{x0} = I_{xb} \dot{p}_b + I_{xc} \dot{p}_c \quad (A37)$$

The transverse angular motion equation is obtained by multiplying the third component of Equation (A35) by i and adding the result to the second component:

$$I_t \dot{Q} - i L_{x0} Q + \dot{\Gamma} + \dot{E} = M_{\tilde{y}} + i M_{\tilde{z}} \quad (A38)$$

where

$$Q = \tilde{q} + i \tilde{r}$$

$$\Gamma = B_\gamma \gamma \exp(i \theta_\gamma)$$

$$E = B_\epsilon \dot{\theta} \epsilon \exp(i \theta_\epsilon)$$

The usual linear aerodynamic moment can be written in the form⁶

$$M_x = (1/2) \rho S \ell V^2 C_{\ell_p} (p_b \ell/V) \quad (A39)$$

$$M_{\tilde{y}} + i M_{\tilde{z}} = (1/2) \rho S \ell V^2 \left\{ \left[(p_b \ell/V) C_{M_{p\alpha}} - i C_{M_\alpha} \right] \tilde{\xi} + C_{M_q} (Q \ell/V) - i C_{M_{\dot{\alpha}}} (\dot{\tilde{\xi}} \ell/V) \right\} \quad (A40)$$

where

$$\xi = \beta + i \tilde{\alpha} = \text{complex angle of attack}$$

A good approximate relation between Q and ξ is⁶

$$i Q = \dot{\xi} + \frac{\rho S V}{2 m} C_{L_\alpha} \xi \quad (A41)$$

The small lift term can be neglected when we use this relation in the roll equation, but that term does have a damping effect on the complex angle of attack equation. Equations (A39-A41) can now be used to write Equations (A36) and (A38) in their final forms:

$$\begin{aligned} I_{xb} \dot{p}_b + I_{xc} \dot{p}_c - A_{\ell p} p_b + B_\gamma \left[(\dot{\beta} \cos \theta_\gamma + \dot{\tilde{\alpha}} \sin \theta_\gamma) \right]_{av} \gamma \\ + B_\epsilon \left[\dot{\theta} (\dot{\beta} \cos \theta_\epsilon + \dot{\tilde{\alpha}} \sin \theta_\epsilon) \right]_{av} \epsilon = 0 \end{aligned} \quad (A42)$$

$$I_t \ddot{\xi} - (A_q + i L_{x0}) \dot{\xi} - (A_\alpha + i A_{p\alpha}) \xi + i (\dot{\Gamma} + \dot{E}) = 0 \quad (A43)$$

where

$$A_{\ell p} = (1/2) \rho S \ell^2 V C_{\ell p}$$

$$A_q = (1/2) \rho S \ell^2 V [C_{M_q} + C_{M_{\dot{\alpha}}} - (I_t/m \ell^2) C_{L_\alpha}]$$

$$A_\alpha = (1/2) \rho S \ell V^2 C_{M_\alpha}$$

$$A_{p\alpha} = (1/2) \rho S \ell^2 V [p_b C_{M_{p\alpha}} + (L_{x0}/m \ell^2) C_{L_\alpha}]$$

Although Equations (A42-A43) were derived for a canted internal component precessing with the angle-of-attack plane, they can be applied to a canted component that is fixed with respect to the body of the shell. For this case,

$$\dot{\theta} = p_b \quad \text{and} \quad \dot{\phi} = 0 . \quad (A44)$$

$$\therefore p_c = p_b \quad (A45)$$

Thus Equations (A42-A43) also are valid for the motion of a shell with mass asymmetry.

APPENDIX B. QUASI-LINEAR SOLUTION OF PITCHING AND YAWING MOTION

The quasi-linear approach assumes that the actual angular motion can be approximated over sections of the trajectory by the epicycle solution of the linearized equation with constant coefficients.

Thus

$$\tilde{\xi} = K_1 e^{i\phi_1} + K_2 e^{i\phi_2} \quad (B1)$$

$$\phi_j = \dot{\phi}_j t + \phi_{j0}$$

Equation (B1) can be substituted in Equation (A43) and the small terms involving \ddot{K}_j omitted:

$$\begin{aligned} I_t (-K_1 \dot{\phi}_1^2 + 2i \dot{\phi}_1 \dot{K}_1) - (A_q + iL_{x0}) (K_1 + i K_1 \dot{\phi}_1) \\ - (A_\alpha + iA_{p_\alpha}) K_1 \\ = -i(\dot{\Gamma} + \dot{E}) e^{-i\phi_1} + \{ \} e^{i\hat{\phi}} \end{aligned} \quad (B2)$$

where $\hat{\phi} = \phi_2 - \phi_1$ and $\{ \}$ is the same expression as on the left side of Equation (B2) with the 1 subscript replaced by a 2 subscript. This second term on the right side of Equation (B2) is periodic with an average value of zero while the left side is constant. We therefore have to average the first term on the right side to obtain its contribution to the quasi-linear frequencies and damping rates. θ_γ and θ_ϵ in Γ and E respectively can be computed from θ using the definition

$$\begin{aligned} e^{i\theta} &= \tilde{\xi}/\delta \\ &= [K_1 e^{i\phi_1} + K_2 e^{i\phi_2}] [K_1^2 + K_2^2 + 2K_1 K_2 \cos \hat{\phi}]^{-1/2} \end{aligned} \quad (B3)$$

When $\exp(i\theta)$ is multiplied by $\exp(-i\phi_1)$, we see that the product is a periodic function of $\hat{\phi}$.

Now

$$\begin{aligned}
 [(e^{i\theta}) \cdot e^{-i\phi_1}]_{av} &= \frac{1}{2\pi} \int_0^{2\pi} (e^{i\theta}) \cdot e^{-i\phi_1} d\hat{\phi} \\
 &= \left\{ \left[\dot{\hat{\phi}} e^{i\theta} e^{-i\phi_1} \right]_0^{2\pi} \right. \\
 &\quad \left. + i\dot{\phi}_1 \int_0^{2\pi} e^{i(\theta-\phi_1)} d\hat{\phi} \right\} / 2\pi \\
 &= i\dot{\phi}_1 [e^{i\theta}]_1
 \end{aligned} \tag{B4}$$

$$\begin{aligned}
 [(\dot{\theta} e^{i\theta}) \cdot e^{-i\phi_1}]_{av} &= \left\{ \left[\dot{\hat{\phi}} \dot{\theta} e^{i\theta} e^{-i\phi_1} \right]_0^{2\pi} \right. \\
 &\quad \left. + \dot{\phi}_1 \int_0^{2\pi} (e^{i\theta}) \cdot e^{-i\phi_1} d\hat{\phi} \right\} / 2\pi \\
 &= i\dot{\phi}_1^2 [e^{i\theta}]_1
 \end{aligned} \tag{B5}$$

where

$$[e^{i\theta}]_j = \frac{1}{2\pi} \int_0^{2\pi} e^{i(\theta-\phi_j)} d\hat{\phi}$$

Equations (B4-B5) can be used in averaging Equation (B2) and the result separated into real and imaginary parts:

$$I_t \dot{\phi}_1^2 - (L_{x0} - C_{11} K^{-1}) \dot{\phi}_1 + A_\alpha = 0 \tag{B6}$$

$$\dot{K}_1 = \lambda_1 K_1 + \dot{\phi}_1 S_1 [2I_t \dot{\phi}_1 - L_{x0}]^{-1} \quad (B7)$$

where

$$C_j = [B_{\gamma j} \gamma \cos \phi_\gamma + B_\epsilon \dot{\phi}_j \epsilon \cos \phi_\epsilon] [e^{i\theta}]_j$$

$$S_j = [B_{\gamma j} \gamma \sin \phi_\gamma + B_\epsilon \dot{\phi}_j \epsilon \sin \phi_\epsilon] [e^{i\theta}]_j$$

$$B_{\gamma j} = I_{xc} p_c - I_{tc} \dot{\phi}_j$$

$$\lambda_j = [A_q \dot{\phi}_j + A_{p\alpha}] [2I_t \dot{\phi}_j - L_{x0}]^{-1}$$

In a similar fashion, the frequencies and damping rates for the second mode can be derived.

$$I_t \dot{\phi}_2^2 - (L_{x0} - C_2 K_2^{-1}) \dot{\phi}_2 + A_\alpha = 0 \quad (B8)$$

$$\dot{K}_2 = \lambda_2 K_2 + \dot{\phi}_2 S_2 [2I_t \dot{\phi}_2 - L_{x0}]^{-1} \quad (B9)$$

Let $\Delta \dot{\phi}_j = \dot{\phi}_j - \dot{\phi}_{jr}$ where $\dot{\phi}_{jr}$ is the j-th frequency of the rigid body consisting of the external body and the internal component. Equations (B6) and (B8) become

$$\begin{aligned} I_t (\dot{\phi}_{jr}^2 + 2 \dot{\phi}_{jr} \Delta \dot{\phi}_j) - L_{x0} (\dot{\phi}_{jr} + \Delta \dot{\phi}_j) \\ + C_j K_j^{-1} \dot{\phi}_{jr} + A_\alpha = 0 \end{aligned} \quad (B10)$$

Thus

$$\Delta \dot{\phi}_j = \frac{-C_j K_j^{-1} \dot{\phi}_{jr}}{2I_t \dot{\phi}_{jr} - L_{x0}} \quad (B11)$$

APPENDIX C. QUASI-LINEAR SOLUTION OF THE ROLL EQUATION

The average of the periodic γ -term in the roll equation (Equation (A42)) can be obtained from the following relations*:

$$\begin{aligned} [\sin (\theta_{\gamma}-\theta_j)]_{av} &= \left[\frac{e^{i[(\theta-\phi_j)+\phi_{\gamma}]} - e^{i[(\phi_j-\theta)-\phi_{\gamma}]} }{2i} \right]_{av} \\ &= [e^{i\theta}]_j \sin \phi_{\gamma} \end{aligned} \quad (C1)$$

$$\begin{aligned} [\dot{\beta} \cos \theta_{\gamma} + \dot{\alpha} \sin \theta_{\gamma}]_{av} &= R\{\dot{\xi} e^{-i\theta_{\gamma}}\}_{av} \\ &= [\dot{\phi}_1 K_1 \sin (\theta_{\gamma}-\phi_1) + \dot{\phi}_2 K_2 \sin (\theta_{\gamma}-\phi_2)]_{av} \\ &= (\dot{\phi}_1 K_1 [e^{i\theta}]_1 + \dot{\phi}_2 K_2 [e^{i\theta}]_2) \sin \phi_{\gamma} \end{aligned} \quad (C2)$$

$$\begin{aligned} [\dot{\theta}(\dot{\beta} \cos \theta_{\gamma} + \dot{\alpha} \sin \theta_{\gamma})]_{av} &= [(\dot{\beta} \sin \theta_{\gamma} - \dot{\alpha} \cos \theta_{\gamma}) \\ &\quad - \ddot{\beta} \sin \theta_{\gamma} + \ddot{\alpha} \cos \theta_{\gamma}]_{av} \\ &= I\{\dot{\xi} e^{-i\theta_{\gamma}}\}_{av} \\ &= [\dot{\phi}_1^2 K_1 \sin (\theta_{\gamma}-\phi_1) + \dot{\phi}_2^2 K_2 \sin (\theta_{\gamma}-\phi_2)]_{av} \\ &= (\dot{\phi}_1^2 K_1 [e^{i\theta}]_1 + \dot{\phi}_2^2 K_2 [e^{i\theta}]_2) \sin \phi_{\gamma} \end{aligned} \quad (C3)$$

Equations (C2-C3) and similar relations for subscript ϵ can now be used to average Equation (A42) which reduces to

$$I_{xb} \dot{p}_b + I_{xc} \dot{p}_c = A_{lp} p_b - \dot{\phi}_1 K_1 S_1 - \dot{\phi}_2 K_2 S_2 \quad (C4)$$

*For the θ 's of this report, $\int e^{i(\theta-\phi_1)} d\hat{\phi} = \int e^{i(\phi_1-\theta)} d\hat{\phi}$

Note that the spin moment depends on $\gamma \sin \phi_\gamma$ and $\epsilon \sin \phi_\epsilon$, the out-of-plane components of $\gamma e^{i\phi_\gamma}$ and $\epsilon e^{i\phi_\epsilon}$. Moreover, only the out-of-plane components appear in the damping rate equations (B7) and (B9). If S_1 and S_2 are positive, their effect is to undamp the fast (K_1) mode, damp the slow (K_2) mode and reduce the spin rate.

DISTRIBUTION LIST

<u>No. of Copies</u>	<u>Organization</u>	<u>No. of Copies</u>	<u>Organization</u>
12	Commander Defense Documentation Center ATTN: DDC-TCA Cameron Station Alexandria, VA 22314	1	Commander US Army Electronics Command ATTN: DRSEL-RD Fort Monmouth, NJ 07703
1	Director Defense Nuclear Agency ATTN: STRA Washington, DC 20305	1	Commander US Army Missile Command ATTN: DRSMI-R Redstone Arsenal, AL 35809
1	Director National Security Agency ATTN: TDL Washington, DC 20301	1	Commander US Army Tank Automotive Development Command ATTN: DRDTA-RWL Warren, MI 48090
1	Commander US Army Materiel Development and Readiness Command ATTN: DRCDMA-ST 5001 Eisenhower Avenue Alexandria, VA 22333	2	Commander US Army Mobility Equipment Research & Development Command ATTN: DRSME-RZT, Tech Docu Cen, Bldg. 315 Fort Belvoir, VA 22060
1	Office of Project Manager US Army Materiel Development and Readiness Command ATTN: DRCPM-NUC Dover, NJ 07801	5	Commander US Army Armament Research and Development Command ATTN: DRDAR-LCA-F, Mr. A. Loeb Mr. S. Wasserman DRDAR-LC-LCN, Mr. W. R. Benson Mr. D. Costa DRDAR-LC-LCU, Mr. A. M. Moss Dover, NJ 07801
1	Commander US Army Aviation Systems Command ATTN: DRSAB-E 12th and Spruce Streets St. Louis, MO 63166		
1	Director US Army Air Mobility Research and Development Laboratory Ames Research Center Moffett Field, CA 94035	1	Commander US Army Yuma Proving Ground ATTN: STEYP-TMW, Mr. R. Fillman Yuma, AZ 85364

DISTRIBUTION LIST

<u>No. of</u> <u>Copies</u>	<u>Organization</u>	<u>No. of</u> <u>Copies</u>	<u>Organization</u>
1	Commander US Army Harry Diamond Labs ATTN: DRXDO-TI 2800 Powder Mill Road Adelphi, MD 20783	1	Commander US Army Research Office ATTN: CRD-AA-EH P.O. Box 12211 Research Triangle Park NC 27709
1	Commander US Army Materials and Mechanics Research Center ATTN: DRXMR-ATL Watertown, MA 02172	2	Commander US Naval Surface Weapons Center ATTN: Code DG40, Dr. W.R. Chadwick Dr. W.G. Soper Dahlgren, VA 22448
1	Commander US Army Training and Doctrine Command ATTN: ATCD-CF, LTC R.E. Camp Fort Monroe, VA 23651	1	Commander US Naval Surface Weapons Center ATTN: Code 730, Tech Lib Silver Spring, MD 20910
1	Director US Army TRADOC Systems Analysis Activity ATTN: ATAA-SA White Sands Missile Range NM 88002	1	Commander US Naval Weapons Center ATTN: Code 753, Lib China Lake, CA 93555
1	Commander US Army Field Artillery School ATTN: ATSF-CD-WC, CPT M. Yap Fort Sill, OK 73503	1	Commander US Naval Research Laboratory ATTN: Tech Info Div Washington, DC 20375
1	Commander US Army Nuclear Agency ATTN: ATCANA-M, MAJ J. Adam Fort Bliss, TX 79916	1	AFATL (Tech Lib) Eglin AFB, FL 32542
1	HQDA (DAMA-CSM-N) Washington, DC 20310	1	AFWL (SUL) Kirtland AFB, NM 87117
1	HQDA (DAMA-DDC) Washington, DC 20310	1	AFFDL Wright-Patterson AFB, OH 45433
1	HQDA (DAMO-ZD, Mr. E. Smith) Washington, DC 20310	1	ASD (ASAMCC) Wright-Patterson AFB, OH 45433

DISTRIBUTION LIST

<u>No. of Copies</u>	<u>Organization</u>
2	Director National Aeronautics and Space Administration Langley Research Center ATTN: MS 185, Tech Lib Dr. Clarence Young Langley Station Hampton, VA 23365
2	Director Sandia Laboratories ATTN: Division 1342, Mr. W.F. Hartman Division 1331, Mr. H.R. Vaughn Albuquerque, NM 87115
1	General Electric Company Armament Systems Department ATTN: Mr. Robert H. Whyte Lakeside Avenue Burlington, VT 05401

Aberdeen Proving Ground

Marine Corps Ln Ofc
Dir, USAMSAA